ITO-Free Flexible Indoor Organic Solar Cells using PEDOT: PSS Conductive Electrode Demonstrating PCE over 10% On a Polyethylene Naphthalate (PEN) Substrate

Jeong-hoon[1], Sung-ho[1], Abdul-aziz Alsalman[2], Hee-Jin Jinho[1], Salman Akram[3]and Ali Raza[3]

[1]School of Electrical and Electronic Engineering, Yonsei University, Seoul 120-749, Republic of Korea.
[2]Department of Chemistry School of Sciences Maulana Azad National Urdu University, Saudi Arabia.
[3]Department of Physics, Lahore University of Management Sciences (LUMS), Lahore, Pakistan

***Abstract* –Solution-processed flexible organic photovoltaics (OPVs) have gained tremendous popularity worldwide during the last two decades. Indium tin oxide (ITO) is commonly used as a transparent conductive electrode in OPVs due to its large conductivity and good transmittance but it is fragile, rigid, and quite expensive. In this paper, flexible solar cells, with Poly (3, 4-ethylenedioxythiophene): poly(styrene-sulfonic acid) (PEDOT: PSS) transparent conductive electrodes are successfully demonstrated on a Polyethylene Naphthalate (PEN) substrate. Prior to PEDOT: PSS electrode, a buffer layer of polyvinyl alcohol (PVA) is added to PEN substrate. The OPV with PEDOT:PSS anode produced power conversion efficiency (PCE) average values of (12.0 % ± 0.1%) while the reference device with ITO exhibited PCE values of (8.0 % ± 0.0%) under a 500-lux-light emitting diode (LED) lamp. Besides PCE improvement, a flexible OPV device also exhibits superior flexibility over ITO as it can retain its PCE up to 85% even after 500 bending cycles in air while the PCE of ITO-based device declined to 15 % of its original value during a similar bending condition. To our knowledge, this excellent bending flexibility and PCE value are the highest recorded, under a 500-lux LED lamp on a PEN substrate.**

Keywords— organic photovoltaics, ITO-free, solution-processed, flexibility, dim lighting conditions.

INTRODUCTION

Organic photovoltaic has become one of the promising sustainable economic solutions as a renewable energy source over the last few decades [1-9]. The solar cell has been widely used in modern applications like robotics, greenhouses, portable electronics, consumer products, and electronic textiles due to its enormous advantages of low-cost, high-throughput, easy fabrication processes for large area solar cells, lightweight and suitable for flexible substrates [10-17].

Apart from the use of solar cells in outdoor environments, many low-power applications such as sensors, chargers, actuators, and wireless sensor nodes (WSN) etc. in houses and offices are also operating under low light conditions [18-25]. The irradiation spectrum and intensity of the light sources used for indoor applications are different from that of under 1-sun [26-28]. Various artificial sources like a light emitting diode (LED), fluorescent lamp, halogen lamp and incandescent lamps are usually used for dim light applications [29-35]. Flexibility is one of the important factors for the commercialization of organic photovoltaic technology in consumer applications [36-37]. Flexible organic devices need a flexible transparent bottom electrode, which should exhibit high conductivity, better mechanical flexibility and transmittance [38-42]. Currently, Indium Tin Oxide (ITO) is a standard transparent bottom electrode widely used in photovoltaic devices but its high cost, low conductivity on plastic substrates, and poor bending capabilities hinder its use for flexible optoelectronic systems [43-47]. There are alternative transparent conductive electrodes such as carbon nanotubes, conductive polymers, silver nanowires, graphene and many others that have been used on different flexible substrates [48-55]. Single-walled carbon nanotube network has been used as transparent electrode with average transmittance and sheet resistance of 85% of 200 Ω/sq respectively [56-58]. Metal Nanowires such as Cu and Ag are also good alternatives of ITO substrate [59-60]. Yang et al. with PCE of 2.5 % using conventional geometry have fabricated AgNw on PET substrate. Their device presented transmittance of 80% with a comparatively lower sheet resistance of 30.8 Ω/sq [61]. In 2016, Wang et al., increased transmission of Cu NWs electrode to 90% by applying hydrogen plasma treatment at room temperature while sheet resistance declined to 19 Ω/sq [62]. Graphene is also an ideal contender for next-generation flexible electrodes due to its mechanical stability, high carrier mobility (2×10^5 cm^2/V_s), low cost, large specific area (2.6×10^3 m^2/g) and better transmittance [63-66].

Conductive polymer like PEDOT: PSS is extensively used polymer for fabrication of solar cells. Different strategies including surface treatment by acids, spin-rinsing, and dry transfer of PEDOT: PSS, has been proposed to increase the electrical conductivity, and optical transmittance of flexible electrode employed by PEDOT: PSS [67-68]. Zhou et al. used a combination of PH500 and PEDOT (EL) as a conductive electrode. The structure of their device was PET/polymer anode/APFO-3: PCBM/LiF/Al, which demonstrated PCE of 2.2 % [69]. All the previously described transparent electrodes are investigated under 1-sun conditions while few issues for example high surface roughness of the electrodes, costly and complex fabrication methods, still exists for the use of these electrodes under low light conditions [70-74]. Recently, we reported ITO-free flexible organic solar cell employing ZnO/Ag/ZnO as the transparent conducting anode for indoor light applications with high optical transmittance up to 92% and very low sheet resistance of 4.8 Ω/sq. The inverted structure (PET/ZnO/Ag/ZnO/PEIE/P3HT: ICBA/MoO_x/Ag).

In the current study, ITO free flexible organic solar cell is fabricated using PEDOT: PSS (PH1000) as transparent anode on a PEN substrate. The flexible device with P3HT: ICBA active layer showed higher power conversion efficiency (PCE) of ~ 11% under 500-lux-LED approximately 25% higher than the reference ITO based device, which exhibits 8% under similar conditions. Furthermore, it shows superior mechanical flexibility over ITO up to 500 bending cycles and can withstand 85% of its PCE at a bending radius of 7.99 mm without mechanical deformation.

Working mechanism and Analysis

The work function values of ITO and PEDOT: PSS electrodes with and without PEIE layer were calculated using Kelvin probe (KP) in ambient air. Highly oriented pyrolytic graphite (HOPG) and ITO_glass were used as a reference which displayed WF values of (5.14 ± 0.058 eV) and (4.87 ± 0.027 eV) respectively. The schematic of the OPV device with an inverted structure is shown in Figure 1.

Fig. 1. Schematic of various participating layers of organic photovoltaic (OPV) device.

The WF value of the reference PEN_ITO was found to be (4.82 ± 0.074 eV) while the anode PEDOT: PSS (PH1000) on PEN substrate exhibited higher WF value of approximately (5.02 ± 0.043 eV). There was a huge difference between the WF values of anodes and electron affinity (EA) (3.57eV) of the acceptor ICBA to provide suitable energy-level alignment [23]. Therefore, to resolve this issue, a buffer layer of PEIE for surface modification was added on both anodes. The inclusion of this PEIE layer, resulted in an improved energy-level alignment of anodes with EA of the ICBA by decreasing the WF values of PEN_ITO and PEN_PEDOT: PSS films to (4.05 ± 0.039 eV) and (4.12 ± 0.054 eV) respectively. The optical transparency of the OPVs presented in Figure 2. Transmittance for PEN_PEDOT: PSS and PEN_ITO in visible spectral range (390-700 nm) is found to be ~ 75 and ~ 85 % respectively. PEN_PEDOT: PSS presented slightly higher transmittance (~70 %) compared to that of PEN_ITO (~65%) in 400-450 nm range.

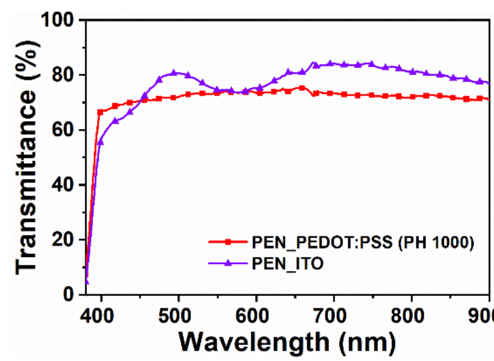

Fig. 2. Transmittance spectra of electrodes.

The J-V curve of both devices under 1-sun and in the dark is depicted in Figure 3. Under 1-sun, PEN-ITO reference device exhibited PCE of (2.3 ± 0.3%) with J_{sc} (6.9 ± 0.8 mA/cm^2) and V_{oc} (826 ± 2 mV). Whereas, the device PEN_PEDOT: PSS showed PCE (1.5 ± 0.1%) and comparatively smaller Jsc (6.3 ± 0.5 mA/cm^2). V_{oc} also drops to (638 ± 24 mV). V_{oc} of

PEN_PEDOT: PSS device is significantly smaller than that of PEN_ITO device under 1-sun, which could be the reason of inferior PCE. V_{oc} of fullerene based OPVs is generally determined by difference between HOMO and LUMO energy levels of donor and acceptor respectively. In this study, the difference in energy levels of PEN_ITO_PEIE (4.05 eV) and PEN_PEDOT:PSS_PEIE (4.12 eV) with ICBA (3.57 eV) is 0.48 and 0.57 eV respectively. Relatively higher difference in energy level of PEN_PEDOT: PSS device compared with that of PEN_ITO, results in smaller V_{oc} followed by decline in PCE under 1-sun. Another reason for smaller V_{oc} could be the higher sheet resistance (R_{CH}) of PEN_PEDOT: PSS because higher sheet resistance (132 Ω/cm^2) could induced the surface recombination instead of drift of charge carriers which results in higher leakage current and smaller $R_{sh}A$ values.

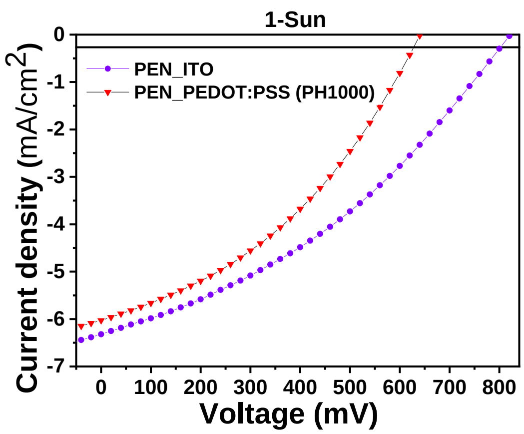

Figure 3. Current-density (J-V) curves under 1-sun.

Regarding J_{sc}, one of the reason for lower current density J_{sc} in PEN_PEDOT: PSS could be the fairly higher R_sA value of (88±12 Ω/cm^2) when compared with R_sA value of PEN_ITO (42±3 Ω/cm^2). To validate, the shrinkage in J_{sc} of PEN_PEDOT: PSS device, the external quantum efficiency (EQE) of both devices was measured by using incident photon-to-current efficiency (IPCE) system as represented by figure 4. EQE spectra of PEN_PEDOT: PSS was little lower than that of reference device which confirms the small difference in the J_{sc} values of both devices under 1-sun. The cross-section view of the OPV device is shown in Figure 5.

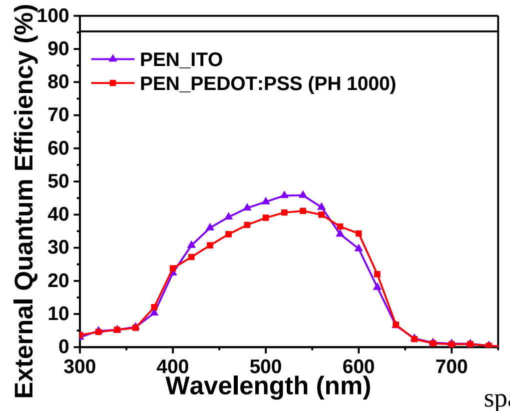

The

spa

Fig. 4. External quantum efficiency (EQE) level of OPV devices.

Bs

O

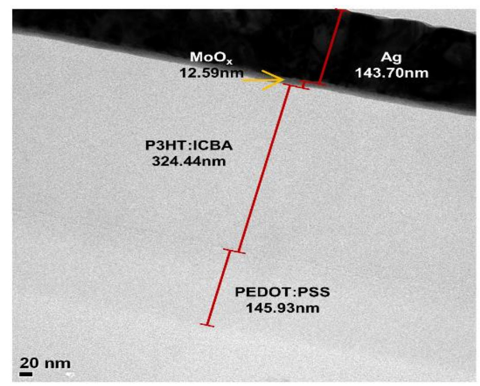

Fig. 5. SEM image of flexible OPV device.

CONCLUSION

In this study, solution-processed BHJ organic solar cells with flexible ITO and PEDOT: PSS (PH 1000) as bottom electrodes are fabricated on PEN substrate successfully. PEN_PEDOT: PSS device exhibited superior performance over PEN_ITO in terms of power conversion efficiency and mechanical durability up to 500 bending cycles under indoor light conditions at different bending curvatures. The optimized PCE values for both PEN_PEDOT: PSS and PEN_ITO devices are (11 % ± 0.1%) and (8% ± 0.1%) under LED respectively. On top of that, PEN_PEDOT:PSS OPV demonstrated excellent mechanical stability compared to PEN_ITO device as it retained its PCE and FF values up to ~85 and ~ 90% respectively even after 500 bending cycles. These results provide an effective pathway toward the use of low-cost ITO-free flexible optoelectronic devices for indoor light applications.

REFERENCES

1. Panwar, N.L., Kaushik, S.C. and Kothari, S., 2011. Role of renewable energy sources in environmental protection: A review. *Renewable and sustainable energy reviews*, *15*(3), pp.1513-1524.

2. Boriskina, S.V., Ghasemi, H. and Chen, G., 2013. Plasmonic materials for energy: From physics to applications. *Materials Today*, *16*(10), pp.375-386.
3. Friji, H., Khanfor, A., Ghazzai, H. and Massoud, Y., 2022. An End-to-End Smart IoT-Driven Navigation for Social Distancing Enforcement. *Ieee Access*, *10*, pp.76824-76841.
4. Khaliq, H.S., Kim, J., Naeem, T., Riaz, K., Badloe, T., Seong, J., Akbar, J., Zubair, M., Mehmood, M.Q., Massoud, Y. and Rho, J., 2022. Broadband Chiro-Optical Effects for Futuristic Meta-Holographic Displays. *Advanced Optical Materials*, p.2201175.
5. Kumar, R., Divyanshu, D., Khan, D., Amara, S. and Massoud, Y., 2022. Spin Orbit Torque-Assisted Magnetic Tunnel Junction-Based Hardware Trojan. *Electronics*, *11*(11), p.1753.
6. Naveed, M.A., Kim, J., Ansari, M.A., Kim, I., Massoud, Y., Kim, J., Oh, D.K., Badloe, T., Lee, J., Kim, Y. and Jeon, D., 2022. Single-Step Fabricable Flexible Metadisplays for Sensitive Chemical/Biomedical Packaging Security and Beyond. *ACS Applied Materials & Interfaces*, *14*(27), pp.31194-31202.
7. Goyal, A.K., Kumar, A. and Massoud, Y., 2022, May. Thermal Stability Analysis of Surface Wave Assisted Bio-Photonic Sensor. In *Photonics* (Vol. 9, No. 5, p. 324). MDPI.
8. Naveed, M.A., Kim, J., Javed, I., Ansari, M.A., Seong, J., Massoud, Y., Badloe, T., Kim, I., Riaz, K., Zubair, M. and Mehmood, M.Q., 2022. Novel Spin-Decoupling Strategy in Liquid Crystal-Integrated Metasurfaces for Interactive Metadisplays. *Advanced Optical Materials*, p.2200196.
9. Khan, M.A., Mehmood, M.Q. and Massoud, Y., 2022. High-Temperature Annealing Effects on Atomically Thin Tungsten Diselenide Field-Effect Transistor. *Applied Sciences*, *12*(16), p.8119.
10. Gulafshan, G., Amara, S., Kumar, R., Khan, D., Fariborzi, H. and Massoud, Y., 2022. Bitwise Logical Operations in VCMA-MRAM. *Electronics*, *11*(18), p.2805.
11. Goyal, A.K., Kumar, A. and Massoud, Y., 2022. Performance Analysis of DAST Material-Assisted Photonic-Crystal-Based Electrical Tunable Optical Filter. *Crystals*, *12*(7), p.992.
12. Bhatti, M.H., Jabbar, M.A., Khan, M.A. and Massoud, Y., 2022. Low-Cost Microwave Sensor for Characterization and Adulteration Detection in Edible Oil. *Applied Sciences*, *12*(17), p.8665.
13. Abbas, M.A., Kim, J., Rana, A.S., Kim, I., Rehman, B., Ahmad, Z., Massoud, Y., Seong, J., Badloe, T., Park, K. and Mehmood, M.Q., 2022. Nanostructured chromium-based broadband absorbers and emitters to realize thermally stable solar thermophotovoltaic systems. *Nanoscale*, *14*(17), pp.6425-6436.
14. Pervez, I., Antoniadis, C. and Massoud, Y., 2022. A Reduced Search Space Exploration Metaheuristic Algorithm for MPPT. *IEEE Access*, *10*, pp.26090-26100.
15. Hamrouni, A., Ghazzai, H., Alelyani, T. and Massoud, Y., 2021. Low-complexity recruitment for collaborative mobile crowdsourcing using graph neural networks. *IEEE Internet of Things Journal*, *9*(1), pp.813-829.
16. Bilal, R.M.H. and Naveed, M.A., 2021. A comment: a set square design metamaterial absorber for X-band applications. Journal of Electromagnetic Waves and Applications, 35(10), pp.1354-1358.
17. Lucic, M.C., Ghazzai, H., Lipizzi, C. and Massoud, Y., 2021. Integrating County-Level Socioeconomic Data for COVID-19 Forecasting in the United States. *IEEE Open Journal of Engineering in Medicine and Biology*, *2*, pp.235-248.
18. Kim, S.H., Sun, C., Saeed, M.A., Kwon, H.J., Kim, T.H., Kwon, S.K., Kim, Y.H. and Shim, J.W., Fine-Tuning of Inner Sidechain of Donor Polymer for Efficient Indoor Organic Photovoltaics. Available at SSRN 4130131.
19. Wan, X., Lucic, M.C., Ghazzai, H. and Massoud, Y., 2021. Topic Modeling and Progression of American Digital News Media During the Onset of the COVID-19 Pandemic. *IEEE Transactions on Technology and Society*.
20. Masmoudi, M., Friji, H., Ghazzai, H. and Massoud, Y., 2021. A reinforcement learning framework for video frame-based autonomous car-following. *IEEE Open Journal of Intelligent Transportation Systems*, *2*, pp.111-127.
21. Khan, M.U., Abbas, M., Khan, M.M., Kousar, A., Alam, M., Massoud, Y. and Jafri, S.H.M., 2021. Modeling and design of low-cost automatic self cleaning mechanism for standalone micro PV systems. *Sustainable Energy Technologies and Assessments*, *43*, p.100922.
22. Friji, H., Hamadi, R., Ghazzai, H., Besbes, H. and Massoud, Y., 2021. A generalized mechanistic model for assessing and forecasting the spread of the COVID-19 pandemic. *Ieee Access*, *9*, pp.13266-13285.
23. Hamadi, R., Ghazzai, H., Besbes, H. and Massoud, Y., 2020. Financial Advisor Recruitment: A Smart Crowdsourcing-Assisted Approach. *IEEE Transactions on Computational Social Systems*, *8*(3), pp.682-688.
24. Wan, X., Lucic, M.C., Ghazzai, H. and Massoud, Y., 2020. Empowering real-time traffic reporting systems with nlp-processed social media data. *IEEE Open Journal of Intelligent Transportation Systems*, *1*, pp.159-175.
25. Bouhamed, O., Ghazzai, H., Besbes, H. and Massoud, Y., 2020. A UAV-assisted data collection for wireless sensor networks: Autonomous navigation and scheduling. *IEEE Access*, *8*, pp.110446-110460.
26. Khan, M.U., Kousar, A., Alam, M. and Massoud, Y., 2020. Closed Form Resonance Solution in Metallic Nanoparticles With Cubic Nonlinearity. *IEEE Transactions on Nanotechnology*, *19*, pp.461-468.
27. Lucic, M.C., Wan, X., Ghazzai, H. and Massoud, Y., 2020. Leveraging intelligent transportation systems and smart vehicles using crowdsourcing: An overview. *Smart Cities*, *3*(2), pp.341-361.
28. Wan, X., Ghazzai, H. and Massoud, Y., 2020. A generic data-driven recommendation system for large-scale regular and ride-hailing taxi services. *Electronics*, *9*(4), p.648.
29. Hamrouni, A., Ghazzai, H. and Massoud, Y., 2020. Many-to-many recruitment and scheduling in spatial mobile crowdsourcing. *IEEE Access*, *8*, pp.48707-48719.
30. Bouhamed, O., Ghazzai, H., Besbes, H. and Massoud, Y., 2020. A generic spatiotemporal scheduling for autonomous UAVs: A reinforcement learning-based approach. *IEEE Open Journal of Vehicular Technology*, *1*, pp.93-106.
31. Dhieb, N., Ghazzai, H., Besbes, H. and Massoud, Y., 2020. A secure ai-driven architecture for automated insurance systems: Fraud detection and risk measurement. *IEEE Access*, *8*, pp.58546-58558.
32. Lucic, M.C., Ghazzai, H. and Massoud, Y., 2020. A generalized dynamic planning framework for green UAV-assisted intelligent transportation system infrastructure. *IEEE Systems Journal*, *14*(4), pp.4786-4797.
33. Hamrouni, A., Ghazzai, H., Frikha, M. and Massoud, Y., 2020. A spatial mobile crowdsourcing framework for event reporting. *IEEE transactions on computational social systems*, *7*(2), pp.477-491.
34. Hanif, A., Mahmood, A., Alam, M. and Massoud, Y., 2019. A compact impedance model of plasmonic nanoshell for metamaterial applications. *IEEE Transactions on Nanotechnology*, *18*, pp.955-962.
35. Wan, X., Ghazzai, H. and Massoud, Y., 2019. Mobile crowdsourcing for intelligent transportation systems: Real-time navigation in urban areas. *IEEE Access*, *7*, pp.136995-137009.
36. Lu, R., Arifuzzman, A.K.M., Hossain, M.K., Gardner, S., Eliza, S.A., Alexander, J.I.D., Massoud, Y. and Haider, M.R., 2019. A Low-Power Sensitive Integrated Sensor System for Thermal Flow Monitoring. *IEEE Transactions on Very Large Scale Integration (VLSI) Systems*, *27*(12), pp.2949-2953.
37. Alam, M., Mahmood, A., Azam, S., Butt, M.S., Haq, A.U. and Massoud, Y., 2019. Impedance model of cylindrical nanowires for metamaterial applications. *Nanomaterials*, *9*(8), p.1104.

38. Kim, T.H., Neu, J.S., Kim, S.H., Saeed, M.A., You, W. and Shim, J.W., 2022. Drastic performance improvement of indoor organic photovoltaics using novel laminated homojunction hole-transport layer. Journal of Materials Chemistry A.
39. Bahabry, A., Wan, X., Ghazzai, H., Menouar, H., Vesonder, G. and Massoud, Y., 2019. Low-altitude navigation for multi-rotor drones in urban areas. *IEEE Access*, *7*, pp.87716-87731.
40. Zhang, T., Haider, M.R., Massoud, Y. and Alexander, J.I.D., 2019. An oscillatory neural network based local processing unit for pattern recognition applications. *Electronics*, *8*(1), p.64.
41. Ghazzai, H., Kadri, A., Ghorbel, M.B., Menouar, H. and Massoud, Y., 2018. A generic spatiotemporal UAV scheduling framework for multi-event applications. *IEEE Access*, *7*, pp.215-229.
42. Lu, R., Haider, M.R., Gardner, S., Alexander, J.I.D. and Massoud, Y., 2018. A paper-based inkjet-printed graphene sensor for breathing-flow monitoring. *IEEE Sensors Letters*, *3*(2), pp.1-4.
43. Saeed, M.A., Bazaz, S.A., Ahmed, N., Naseem, M. and Rehman, A., 2016, December. Design and simulation of microchannel for DNA amplification. In 2016 19th International Multi-Topic Conference (INMIC) (pp. 1-5). IEEE.
44. Gardner, S.D., Alexander, J.I.D., Massoud, Y. and Haider, M.R., 2020, December. Minimally produced inkjet-printed tactile sensor model for improved data reliability. In *2020 11th International Conference on Electrical and Computer Engineering (ICECE)* (pp. 49-52). IEEE.
45. Friji, H., Ghazzai, H., Besbes, H. and Massoud, Y., 2020, December. A DQN-based autonomous car-following framework using RGB-D frames. In *2020 IEEE Global Conference on Artificial Intelligence and Internet of Things (GCAIoT)* (pp. 1-6). IEEE.
46. Khanfor, A., Friji, H., Ghazzai, H. and Massoud, Y., 2020, December. A social iot-driven pedestrian routing approach during epidemic time. In *2020 IEEE Global Conference on Artificial Intelligence and Internet of Things (GCAIoT)* (pp. 1-6). IEEE.
47. Hamrouni, A., Ghazzai, H., Alelyani, T. and Massoud, Y., 2020, December. An Evolutionary Algorithm for Collaborative Mobile Crowdsourcing Recruitment in Socially Connected IoT Systems. In *2020 IEEE Global Conference on Artificial Intelligence and Internet of Things (GCAIoT)* (pp. 1-6). IEEE.
48. Bouhamed, O., Ghazzai, H., Besbes, H. and Massoud, Y., 2020, October. Autonomous UAV navigation: A DDPG-based deep reinforcement learning approach. In *2020 IEEE International Symposium on Circuits and Systems (ISCAS)* (pp. 1-5). IEEE.
49. Khanfor, A., Nammouchi, A., Ghazzai, H., Yang, Y., Haider, M.R. and Massoud, Y., 2020, August. Graph neural networks-based clustering for social internet of things. In *2020 IEEE 63rd International Midwest Symposium on Circuits and Systems (MWSCAS)* (pp. 1056-1059). IEEE.
50. Saeed, M.A., Shahzad, A., Rasool, K., Mateen, F., Oh, J.M. and Shim, J.W., 2022. 2D MXene: A Potential Candidate for Photovoltaic Cells? A Critical Review. Advanced Science, 9(10), p.2104743.
51. Gardner, S.D., Alexander, J.I.D., Massoud, Y. and Haider, M.R., 2020, October. An Inkjet-Printed Paper-Based Flexible Sensor for Pressure Mapping Applications. In *2020 IEEE International Symposium on Circuits and Systems (ISCAS)* (pp. 1-5). IEEE.
52. Kirolos, S., Laska, J., Wakin, M., Duarte, M., Baron, D., Ragheb, T., Massoud, Y. and Baraniuk, R., 2006, October. Analog-to-information conversion via random demodulation. In *2006 IEEE Dallas/CAS Workshop on Design, Applications, Integration and Software* (pp. 71-74). IEEE.
53. Laska, J.N., Kirolos, S., Duarte, M.F., Ragheb, T.S., Baraniuk, R.G. and Massoud, Y., 2007, May. Theory and implementation of an analog-to-information converter using random demodulation. In *2007 IEEE International Symposium on Circuits and Systems* (pp. 1959-1962). IEEE.
54. Laska, J., Kirolos, S., Massoud, Y., Baraniuk, R., Gilbert, A., Iwen, M. and Strauss, M., 2006, October. Random sampling for analog-to-information conversion of wideband signals. In *2006 IEEE Dallas/CAS Workshop on Design, Applications, Integration and Software* (pp. 119-122). IEEE.
55. Davenport, M.A., Duarte, M.F., Wakin, M.B., Laska, J.N., Takhar, Bilal, R.M.H., Saeed, M.A., Choudhury, P.K., Baqir, M.A., Kamal, W., Ali, M.M. and Rahim, A.A., 2020. Elliptical metallic rings-shaped fractal metamaterial absorber in the visible regime. *Scientific reports*, *10*(1), pp.1-12.
56. Hosseini, A. and Massoud, Y., 2007. Nanoscale surface plasmon based resonator using rectangular geometry. *Applied Physics Letters*, *90*(18), p.181102.
57. Hosseini, A. and Massoud, Y., 2006. A low-loss metal-insulator-metal plasmonic bragg reflector. *Optics express*, *14*(23), pp.11318-11323.
58. Ullah, M.A. and Saeed, M.A., 2014. Design and implementation of efficient elevator control system using fpga. International Journal of Innovation and Applied Studies, 9(4), p.1541.
59. Bilal, R.M.H., Baqir, M.A., Choudhury, P.K., Karaaslan, M., Ali, M.M., Altıntas, O., Rahim, A.A., Unal, E. and Sabah, C., 2021. Wideband microwave absorber comprising metallic split-ring resonators surrounded with E-shaped fractal metamaterial. *IEEE Access*, *9*, pp.5670-5677..
60. Massoud, Y., Majors, S., Bustami, T. and White, J., 1998, May. Layout techniques for minimizing on-chip interconnect self inductance. In *Proceedings of the 35th annual Design Automation Conference* (pp. 566-571).
61. Saeed, M.A., Kim, S.H., Kim, H., Liang, J., Woo, H.Y., Kim, T.G., Yan, H. and Shim, J.W., 2021. Indoor organic photovoltaics: optimal cell design principles with synergistic parasitic resistance and optical modulation effect. *Advanced Energy Materials*, *11*(27), p.2003103.
62. Khan, M.U., Wali, K., Karimov, K.S. and Saeed, M.A., 2015, December. A new proposed hierarchy for renewable energy generation to distribution grid integration. In 2015 International Conference on Emerging Technologies (ICET) (pp. 1-6). IEEE.
63. Bilal, R.M.H., Naveed, M.A., Baqir, M.A., Ali, M.M. and Rahim, A.A., 2020. Design of a wideband terahertz metamaterial absorber based on Pythagorean-tree fractal geometry. *Optical Materials Express*, *10*(12), pp.3007-3020.
64. Baraniuk, R., Baron, D.Z., Duarte, M.F., Elnozahi, M., Wakin, M.B., Davenport, M.A., Laska, J.N., Tropp, J.A., Massoud, Y., Kirolos, S. and Ragheb, T., 2014. *Method and apparatus for on-line compressed sensing*. U.S. Patent 8,687,689.
65. Ragheb, T., Laska, J.N., Nejati, H., Kirolos, S., Baraniuk, R.G. and Massoud, Y., 2008, August. A prototype hardware for random demodulation based compressive analog-to-digital conversion. In *2008 51st Midwest Symposium on Circuits and Systems* (pp. 37-40). IEEE.
66. Kim, T.H., Lee, H.J., Saeed, M.A., Son, J.H., Woo, H.Y., Kim, T.G and Shim, J.W., 2022. Elastomeric Indoor Organic Photovoltaics with Superb Photothermal Endurance. Advanced Functional Materials, p.2201921.
67. Bilal, R.M.H., Baqir, M.A., Choudhury, P.K., Naveed, M.A., Ali, M.M. and Rahim, A.A., 2020. Ultrathin broadband metasurface-based absorber comprised of tungsten nanowires. *Results in Physics*, *19*, p.103471.
68. Hosseini, A., Nejati, H. and Massoud, Y., 2008. Modeling and design methodology for metal-insulator-metal plasmonic Bragg reflectors. *Optics express*, *16*(3), pp.1475-1480.
69. Nieuwoudt, A. and Massoud, Y., 2008. On the optimal design, performance, and reliability of future carbon nanotube-based interconnect solutions. *IEEE transactions on electron devices*, *55*(8), pp.2097-2110.
70. Kirolos, S., Ragheb, T., Laska, J., Duarte, M.F., Massoud, Y. and Baraniuk, R.G., 2006, December. Practical issues in implementing analog-to-information converters. In *2006 6th International*

Workshop on System on Chip for Real Time Applications (pp. 141-146). IEEE.
71. Major, S. and Chopra, K.L., 1988. Indium-doped zinc oxide films as transparent electrodes for solar cells. Solar Energy Materials, 17(5), pp.319-327.
72. Zhang, Y., Ng, S.W., Lu, X. and Zheng, Z., 2020. Solution-processed transparent electrodes for emerging thin-film solar cells. Chemical reviews, 120(4), pp.2049-2122.
73. Morgenstern, F.S., Kabra, D., Massip, S., Brenner, T.J., Lyons, P.E., Coleman, J.N. and Friend, R.H., 2011. Ag-nanowire films coated with ZnO nanoparticles as a transparent electrode for solar cells. Applied Physics Letters, 99(18), p.242.
74. Wu, J., Becerril, H.A., Bao, Z., Liu, Z., Chen, Y. and Peumans, P., 2008. Organic solar cells with solution-processed graphene transparent electrodes. Applied physics letters, 92(26), p.237.